

# Electronic structure of CsFe<sub>2</sub>Sb<sub>2</sub> and its alloy with cobalt: A magnetic compound related to the iron superconductors

Lijun Zhang and D. J. Singh

*Materials Science and Technology Division, Oak Ridge National Laboratory, Oak Ridge, Tennessee 37831-6114, USA*

(Received 8 March 2010; revised manuscript received 28 April 2010; published 17 May 2010)

Properties of ThCr<sub>2</sub>Si<sub>2</sub>-structure CsFe<sub>2</sub>Sb<sub>2</sub> and its alloy with Co are investigated using first principles calculations. CsFe<sub>2</sub>Sb<sub>2</sub> is an antiferromagnetic metal at the density functional level. The electronic structure is closely related to the Fe-based superconductors. Results are discussed in relation to the Fe-based superconductors.

DOI: [10.1103/PhysRevB.81.193102](https://doi.org/10.1103/PhysRevB.81.193102)

PACS number(s): 74.25.Jb, 74.70.Dd, 71.18.+y, 74.25.Kc

The discovery of superconductivity in layered Fe compounds<sup>1,2</sup> has attracted substantial interest both aimed at the discovery of related compounds and at understanding the origins of this behavior. Subsequent work has revealed a rich chemistry and a remarkable interplay between magnetism and superconductivity. The phase diagrams show a competition between an antiferromagnetic, spin density wave (SDW) ordering and superconductivity.<sup>3,4</sup> In Fe pnictides with SDW order, superconductivity often appears when the magnetic order is suppressed by doping, alloying, or pressure, although the two orders can coexist. There is strong evidence for unusually strong spin fluctuations in both the SDW ordered and superconducting Fe pnictides.<sup>5-8</sup> Furthermore a magnetically paired sign changing *s* wave state has been proposed<sup>9</sup> and appears to be supported by experimental data including observation of the corresponding resonance peak in inelastic neutron scattering.<sup>10</sup>

Turning to the chemistry, there are several superconducting families known. Of these, the “122,” ThCr<sub>2</sub>Si<sub>2</sub> structure<sup>11</sup> is the most flexible in the sense that this structure-type can be stabilized by different bonding patterns, with the result that an exceptionally large number of intermetallic compounds occur in it.<sup>12</sup> For example, BaT<sub>2</sub>As<sub>2</sub> forms for almost all *T*=transition element, and several of them have interesting properties, such as magnetism or superconductivity.<sup>13</sup> Further, doping by alloying on the Fe site can be used to induce superconductivity in BaFe<sub>2</sub>As<sub>2</sub> and SrFe<sub>2</sub>As<sub>2</sub>.<sup>14,15</sup> Density-functional calculations of the electronic structure of these materials show dominant Fe *d* character near the Fermi energy, semimetallic band structures with disconnected Fermi surfaces, and high densities of states that place these materials near itinerant magnetism.<sup>16,17</sup> Importantly, the Fe-pnictide superconductors are rather ionic with the *p* states of As well below the Fermi energy, corresponding to As<sup>3-</sup> and leading to the Fe<sup>2+</sup> metallic sheets, although it should be emphasized that there is As-Fe hybridization that plays an important role in the formation of the energy bands.

One trend in the superconducting properties of the Fe pnictides is that the arsenides generally have higher critical temperatures than the phosphides. Therefore, one might ask what the properties of the corresponding antimonides are.<sup>18</sup> Unfortunately, Sb-based chemical models analogous to the Fe-As superconductors have not been available and instead other competing phases with covalent bonding such as skutterudite tend to form. However, there is one exception. This

is CsFe<sub>2</sub>Sb<sub>2</sub>, which was reported to form in the ThCr<sub>2</sub>Si<sub>2</sub> structure with lattice parameters, *a*=4.0737 Å and *c*=14.8384 Å, by Noack and Schuster.<sup>19</sup> These authors also reported CsFe<sub>2</sub>As<sub>2</sub> in the ThCr<sub>2</sub>Si<sub>2</sub> structure with lattice parameters *a*=3.894 Å and *c*=14.798 Å. Therefore the Fe-Fe spacing in square lattice planes of the antimonide is ~5% larger than in the arsenide, which may be important considering the importance of Fe-Fe hopping in the formation of the electronic structure of the Fe-superconductors.<sup>16,17</sup> Unfortunately, the phase is reactive and besides its lattice parameters little is known about its physical properties.

Here we report some properties based on density functional calculations. These were done using the linearized augmented planewave (LAPW) method<sup>20</sup> and with the projector augmented planewave (PAW) method. The PAW calculations were done using the VASP code,<sup>21</sup> while the LAPW calculations were done using an in-house code as well as the WIEN2K package.<sup>22</sup> The LAPW method was used for the electronic structures and other properties reported here, except as noted. We employed LAPW spheres of radius 2.2 Bohr for all atoms, and computational parameters similar to our prior work on ThCr<sub>2</sub>Si<sub>2</sub>-structure Fe-based superconductors.<sup>23</sup> We used the experimental lattice parameters, and determined the Sb position by energy minimization. Without magnetism the local density approximation (LDA) value is *z*<sub>Sb</sub>=0.3856.

The LDA band structure and electronic density of states for the non-spin-polarized case are shown in Figs. 1 and 2, respectively. As may be seen, the density of states (DOS) near the Fermi energy is derived mainly from Fe *d* states and there is a dip in the DOS at an electron count of six per Fe, which for this material is above *E*<sub>F</sub>. These features are qualitatively similar to results for the Fe-pnictide superconductors. The non-spin-polarized Fermi surface is given in the top panel of Fig. 3. This is similar to that for KFe<sub>2</sub>As<sub>2</sub>, which has the same valence electron count,<sup>24,25</sup> except that the small electron Fermi surface at the zone corner for KFe<sub>2</sub>As<sub>2</sub> is absent in CsFe<sub>2</sub>Sb<sub>2</sub>, since the corresponding bands (see Fig. 1) almost but do not quite reach the Fermi energy, *E*<sub>F</sub>. The hole Fermi surfaces around  $\Gamma$  have an aggregate volume of 1/2 of the zone, corresponding to the one hole introduced on replacing, e.g., Ba by Cs. Interestingly, KFe<sub>2</sub>As<sub>2</sub>, with its small electron sheet is a superconductor, albeit the *T*<sub>c</sub> is low presumably because of the strong overdoping and corresponding small size of the electron sheet.

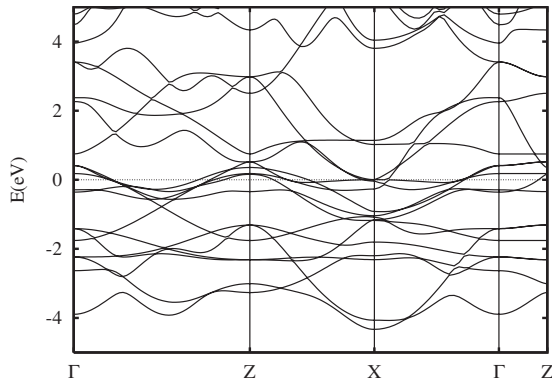


FIG. 1. Calculated LDA band structure of non-spin-polarized  $\text{CsFe}_2\text{Sb}_2$ . The lines show separate  $c$  axis and in-plane dispersions in the bct zone. Z is  $(0,0,1/2)$ , which is also called  $M$ . The short  $\Gamma$ -Z line is along  $k_z$ , the long  $\Gamma$ -Z line is along Cartesian  $(k_x, 0, 0)$  to Z in the next zone, while  $\Gamma$ -X is along the Cartesian  $(k, k, 0)$  direction. If there were no  $c$ -axis dispersion, the bands would be flat along the short  $\Gamma$ -Z line, would have reflection symmetry about the midpoint of the long  $\Gamma$ -Z line, and would be the same along  $X$ -Z and  $X$ - $\Gamma$ .

The value of the non-spin-polarized density of states at  $E_F$  is  $N(E_F)=5.9 \text{ eV}^{-1}$  on a per formula unit basis. This high number favors magnetism. Even in the LDA the ground state is magnetic. We find that the non-spin-polarized solution is unstable against ferromagnetism in the LDA with spin magnetization of  $0.73\mu_B$  per Fe, and Fe moments as measured by the polarization in an Fe LAPW sphere of  $0.84\mu_B$  (note that there is a small back polarization of the Sb). There is an even stronger instability against nearest-neighbor antiferromagnetism.

In order to better characterize the magnetism, we performed PAW calculations for various magnetic configurations. These were ferromagnetic (FM) order, checkerboard (nearest-neighbor antiferromagnetism) ordering (C-AF), so called double stripe antiferromagnetism as observed in FeTe ordering (DS-AF), and the so-called stripe ordering, which is the pattern of the SDW (S-AF).

In all cases except FM the layer stacking was chosen to have alternating spin directions along the  $c$  axis. Calculations were performed both within a scalar relativistic approxima-

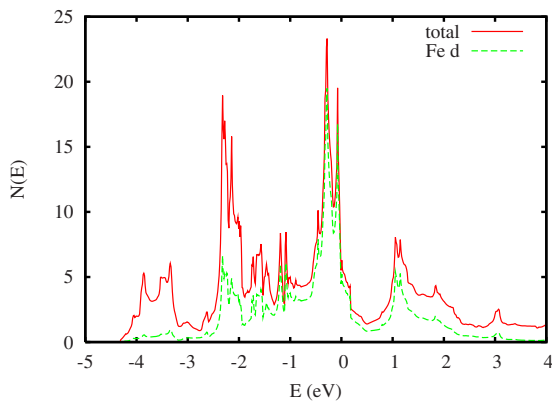


FIG. 2. (Color online) Calculated LDA density of states and Fe  $d$  projection onto the Fe LAPW sphere, radius 2.2 Bohr, for non-spin-polarized  $\text{CsFe}_2\text{Sb}_2$ .

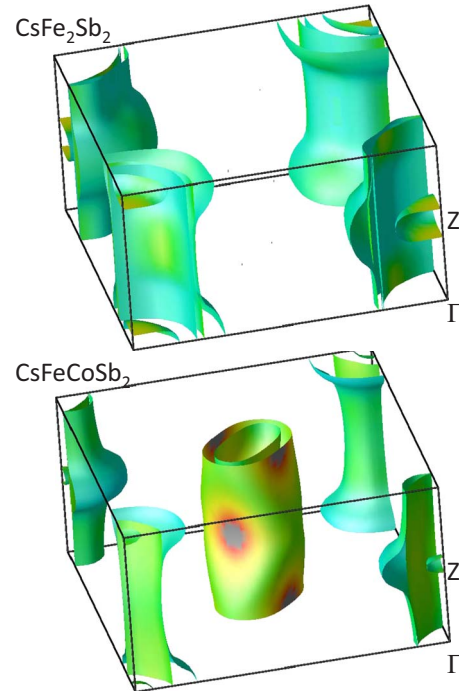


FIG. 3. (Color online) Calculated LDA non-spin-polarized Fermi surfaces for  $\text{CsFe}_2\text{Sb}_2$  and ordered  $\text{CsFeCoSb}_2$  (see text). The shading is by Fermi velocity.

tion and including spin orbit. We also performed calculations both in the LDA and using the generalized gradient approximation (GGA) of Perdew *et al.*<sup>26</sup> The resulting magnetic energies, defined as the difference in energy between the magnetically ordered state and the non-spin-polarized case, calculated in the same way are given in Table I.

As may be seen, the GGA calculations yield much stronger magnetism than the LDA calculations, especially when relaxation of the Sb position is included. This is similar to the Fe-arsenide superconductors.<sup>5</sup> As in FeTe,<sup>27</sup> spin orbit is important in the energetics, presumably reflecting the higher atomic number of Sb compared with As. In the following we focus on the GGA results including spin orbit. The predicted ground state has the double stripe ordering as in FeTe, with Fe moments of  $2.2\mu_B$ . There is an instability of the non-spin-polarized state for SDW type ordering, but it is relatively weak, and in particular the checkerboard nearest-neighbor ordering is lower in energy. This might be expected considering that this compound is over doped in the sense of lacking electron sheets of Fermi surface that are responsible for the nesting driven SDW in the iron pnictides. The magnetically ordered states are all metallic with substantial  $N(E_F)$ . There is prominent splitting of the DOS for the SDW type (S) ordering, but this splitting occurs above  $E_F$  by approximately  $1e$  per unit cell and therefore is not effective in stabilizing the state.

Therefore, based on the electronic structure calculations,  $\text{CsFe}_2\text{Sb}_2$  is an antiferromagnetic metal. At the GGA level the expected ground state is the DS structure, as in FeTe, but we note that the energy difference between the C and DS orderings is small. Similar to the iron arsenide materials<sup>5</sup> the magnetism is rather sensitive to the exchange correlation

TABLE I. The calculated magnetic energy,  $E_{\text{mag}}$  in meV and moment,  $m_{\text{Fe}}$  in  $\mu_B$  for various magnetic orders of  $\text{CsFe}_2\text{Sb}_2$  with the PAW method. Both LDA and GGA exchange-correlation functionals are employed. The energies are given on a per Fe basis. We show results calculated both with non-spin-polarized optimized internal atomic coordinates ( $F$ ), and fully relaxing the internal coordinates for each given magnetic order ( $R$ ). The energies calculated including spin orbit are shown within brackets.

			FM	C-AF	S-AF	DS-AF
LDA	$F$	$E_{\text{mag}}$	-21	-27	-10	-20
		$m_{\text{Fe}}$	0.7	1.3	0.9	1.1
	$R$	$E_{\text{mag}}$	-22	-30	-22	-28
		$m_{\text{Fe}}$	0.7	1.5	1.3	1.3
GGA	$F$	$E_{\text{mag}}$	-60 (-2)	-145 (-81)	-95 (-32)	-121 (-58)
		$m_{\text{Fe}}$	1.0	2.0	1.9	1.8
	$R$	$E_{\text{mag}}$	-69 (-8)	-171 (-108)	-125 (-63)	-182 (-120)
		$m_{\text{Fe}}$	1.1	2.2	2.2	2.2

functional and is very much weaker in the LDA. This may be indicative of an instability of the iron magnetism again similar to the arsenides. Also, it should be noted that in the arsenides, GGA calculations predict rather strong magnetism, while the experimentally determined ordered moments are much smaller. On the other hand, LDA calculations yield structural parameters that place the As too close to the Fe plane along with weaker magnetism that is closer to, but not in quantitative agreement with experiment. One explanation is that there are strong spin fluctuations that renormalize the static GGA ground state suppressing ordering, while retaining the influence of magnetism on bonding.<sup>5,6,17</sup> While type of behavior is very uncommon, based on the similarity of the calculated behavior of  $\text{CsFe}_2\text{Sb}_2$  with that of the arsenides, it may also be the case here.

In view of the above, it will be of interest to explore chemical ways of doping the compound in order to determine whether the magnetic order can be suppressed and whether it will be superconducting in that case. A natural choice would be alloying on the Cs site with a divalent. However,  $\text{BaFe}_2\text{Sb}_2$  is not a known  $\text{ThCr}_2\text{Si}_2$ -structure compound. Therefore it may be very difficult to alloy on the Cs site. Here we considered alloying on the Fe site with Co. This is known to be an effective way to electron dope  $\text{BaFe}_2\text{As}_2$ ,<sup>14</sup> even though electron doping on the Ba site (e.g., with La) has not been reported.  $\text{CsCo}_2\text{Sb}_2$  is not a reported compound to our knowledge. However, we presume that there is some solubility of Co in  $\text{CsFe}_2\text{Sb}_2$ . The question then is whether the electronic structure of the Co-doped antimonide behaves similarly to the arsenides.

To address this we performed LDA calculations for the 50-50 alloy, and compared a virtual crystal calculation and a calculation with an ordered structure formed by replacing one of the Fe atoms in the unit cell by a Co. This composition has one extra electron per unit cell compared to  $\text{CsFe}_2\text{Sb}_2$ , i.e., the same valence electron count as  $\text{BaFe}_2\text{As}_2$ . It was found the electronic structure behaved as a coherent alloy in studies of  $\text{Ba}(\text{Fe},\text{Co})_2\text{As}_2$ .<sup>14</sup> In particular, projections of the DOS on the Fe and Co sites in supercells were similar, and virtual crystal and supercell calculations yielded very nearly the same electronic structures. We followed the

same approach here. Calculations were done with the crystal structure fixed to that of  $\text{CsFe}_2\text{Sb}_2$  for ordered  $\text{CsFeCoSb}_2$  and a virtual crystal  $\text{CsM}_2\text{Sb}_2$ , where  $M$  is a virtual atom with nuclear charge,  $Z_M=26.5$ .

The Fermi surface for the ordered cell is shown in the lower panel of Fig. 3, while the DOS of the ordered and virtual crystal cells is shown in Fig. 4. The Fermi surface for the virtual crystal was very similar to that of the ordered cell and is not shown. The calculated Fermi surface shows disconnected electron and hole sections with the same overall structure as in the arsenide superconductors. Also the DOS

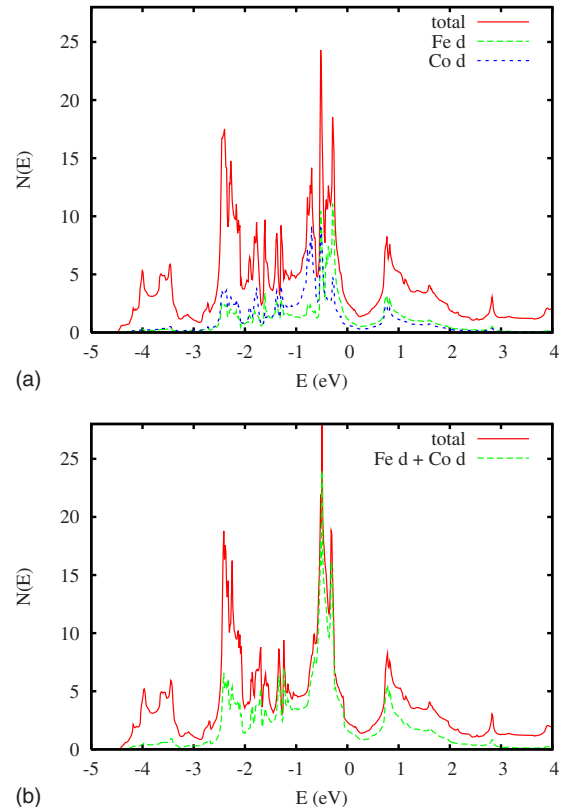


FIG. 4. (Color online) Calculated LDA DOS for ordered  $\text{CsFeCoSb}_2$  (top) and a virtual crystal for the 50-50 alloy (bottom).

for the virtual crystal and ordered cells are similar to each other, as was found in the case of the arsenide.<sup>14</sup> Furthermore, in the ordered cell the Fe and Co projections of the DOS have similar shape, although it may be noted the Co contribution at  $E_F$  is lower than the Fe contribution. This reduced Co DOS leads to a less magnetic system than  $\text{BaFe}_2\text{As}_2$ . Within the LDA we do not find an SDW ground state for  $\text{CsFeCoSb}_2$ . This is similar to the behavior of  $\text{KFeCoAs}_2$  at the LDA level.<sup>24</sup>

In summary, density functional calculations for  $\text{CsFe}_2\text{Sb}_2$  show an electronic structure and magnetic properties that are similar to those of the iron arsenide compounds when calculated at the same level. It will be of interest first of all to determine the magnetic properties of stoichiometric  $\text{CsFe}_2\text{Sb}_2$ . A key question is whether the magnetism will be strong similar to the GGA predictions as opposed to sup-

pressed, as in the iron arsenide superconductors. Second, it will be of interest to study the behavior of electron-doped  $\text{CsFe}_2\text{Sb}_2$  to determine if it becomes a superconductor in analogy with the arsenides, and if so what its superconducting properties are. According to the present calculations, alloying with Co produces a coherent electronic structure and so this is one possibility for electron doping (in analogy with the arsenides Ni may behave similarly). However, we note that unlike the arsenides the end-point Co and Ni compounds have not been reported and therefore the solubility range in  $\text{ThCr}_2\text{Si}_2$ -structure  $\text{CsFe}_2\text{Sb}_2$  may be limited.

We are grateful for helpful discussions with C. Felser, D. Mandrus, M. McGuire, B. C. Sales, and A. S. Sefat. This work was supported by the Department of Energy, Division of Materials Sciences and Engineering.

- 
- <sup>1</sup>Y. Kamihara, H. Hiramatsu, M. Hirano, R. Kawamura, H. Yanagi, T. Kamiya, and H. Hosono, *J. Am. Chem. Soc.* **128**, 10012 (2006).
- <sup>2</sup>Y. Kamihara, T. Watanabe, M. Hirano, and H. Hosono, *J. Am. Chem. Soc.* **130**, 3296 (2008).
- <sup>3</sup>C. de la Cruz *et al.*, *Nature (London)* **453**, 899 (2008).
- <sup>4</sup>G. F. Chen, Z. Li, D. Wu, G. Li, W. Z. Hu, J. Dong, P. Zheng, J. L. Luo, and N. L. Wang, *Phys. Rev. Lett.* **100**, 247002 (2008).
- <sup>5</sup>I. I. Mazin, M. D. Johannes, L. Boeri, K. Koepernik, and D. J. Singh, *Phys. Rev. B* **78**, 085104 (2008).
- <sup>6</sup>I. I. Mazin and M. D. Johannes, *Nat. Phys.* **5**, 141 (2009).
- <sup>7</sup>F. Bondino *et al.*, *Phys. Rev. Lett.* **101**, 267001 (2008).
- <sup>8</sup>F. Ning, K. Ahilan, T. Imai, A. S. Sefat, R. Jin, M. A. McGuire, B. C. Sales, and D. Mandrus, *J. Phys. Soc. Jpn.* **78**, 013711 (2009).
- <sup>9</sup>I. I. Mazin, D. J. Singh, M. D. Johannes, and M.-H. Du, *Phys. Rev. Lett.* **101**, 057003 (2008).
- <sup>10</sup>A. D. Christianson *et al.*, *Nature (London)* **456**, 930 (2008).
- <sup>11</sup>M. Rotter, M. Tegel, and D. Johrendt, *Phys. Rev. Lett.* **101**, 107006 (2008).
- <sup>12</sup>W. B. Pearson, *J. Solid State Chem.* **56**, 278 (1985).
- <sup>13</sup>A. S. Sefat, D. J. Singh, R. Jin, M. A. McGuire, B. C. Sales, and F. Roning, *Physica C* **469**, 350 (2009).
- <sup>14</sup>A. S. Sefat, R. Jin, M. A. McGuire, B. C. Sales, D. J. Singh, and D. Mandrus, *Phys. Rev. Lett.* **101**, 117004 (2008).
- <sup>15</sup>A. Leithe-Jasper, W. Schnelle, C. Geibel, and H. Rosner, *Phys. Rev. Lett.* **101**, 207004 (2008).
- <sup>16</sup>D. J. Singh and M.-H. Du, *Phys. Rev. Lett.* **100**, 237003 (2008).
- <sup>17</sup>D. J. Singh, *Physica C* **469**, 418 (2009).
- <sup>18</sup>L. Zhang, A. Subedi, D. J. Singh, and M. H. Du, *Phys. Rev. B* **78**, 174520 (2008).
- <sup>19</sup>M. Noack and H. U. Schuster, *Z. Anorg. Allg. Chem.* **620**, 1777 (1994).
- <sup>20</sup>D. J. Singh and L. Nordstrom, *Planewaves Pseudopotentials and the LAPW Method*, 2nd ed. (Springer, Berlin, 2006).
- <sup>21</sup>G. Kresse and D. Joubert, *Phys. Rev. B* **59**, 1758 (1999).
- <sup>22</sup>P. Blaha, K. Schwarz, G. Madsen, D. Kvasnicka, and J. Luitz, *WIEN2k, An Augmented Plane Wave+Local Orbitals Program for Calculating Crystal Properties* (K. Schwarz Technical University, Wien, Austria, 2001).
- <sup>23</sup>D. J. Singh, *Phys. Rev. B* **78**, 094511 (2008).
- <sup>24</sup>D. J. Singh, *Phys. Rev. B* **79**, 174520 (2009).
- <sup>25</sup>T. Sato *et al.*, *Phys. Rev. Lett.* **103**, 047002 (2009).
- <sup>26</sup>J. P. Perdew, K. Burke, and M. Ernzerhof, *Phys. Rev. Lett.* **77**, 3865 (1996).
- <sup>27</sup>M. D. Johannes and I. I. Mazin, *Phys. Rev. B* **79**, 220510(R) (2009).